

Supplementary Material 1: English translation of Román and Deza (1998), which briefly describes UCTL methods.

Román, Á. and Á. Deza. 1998. Appendix: Archaeological luminescence dates. In *Arqueología de Mendoza. Las dataciones absolutas y sus alcances*, by J. R. Bárcena, pp. 399–407. Translated by Erik J. Marsh. Editorial de la Universidad Nacional de Cuyo, Mendoza.

Appendix

Archaeological Luminescence Dates

Álvaro Román B. and Ángel D. Deza T.
Facultad de Física, Pontificia Universidad Católica de Chile

Dating ceramics by luminescence was initially suggested by the US physicist Farrington Daniels (1953), who proposed applying thermoluminescence (TL) to date rocks and ancient ceramics. Since then, there have been a series of investigations based on Daniels' idea, carried out in many places, mostly in the US and western Europe. Their successes have made it possible to include TL among the most effective methods used in archeological chronologies.

Brief description of the thermoluminescence phenomenon

TL is a phenomenon tied to solid-state physics, based on light emissions by certain crystalline phosphorescent materials during temperature increases. Emitted light is the consequence of a thermal liberation of energy accumulated inside the crystal after it has been subjected to ionizing radiation. The phenomenon can be explained through the following model: an electron liberated by ionizing radiation travels to the interior of the crystal where it can be trapped by defects in the crystalline structure, called traps. It is possible the electrons remain there for a constant amount of time called a half-life. If this is long, the electron can remain trapped in the crystalline network for an extended period and will not leave this state if it does not receive energy. Adequate thermal stimulation moves electrons to the luminescent centers of

the crystal, producing a TL light emission, which is proportional to the radiation dose absorbed by the substance.

In the interior of the crystal, there can be a number of levels of traps, which have different half-lives that required different amounts of energy to be *emptied*. When the material is irradiated, the crystalline traps are populated with electrons and a progressive increase in temperature empties them, resulting in a light emission that is characteristic of each individual group of traps. With the right equipment, it is possible to simultaneously record the temperature of the crystal and the light emission, thereby obtaining a TL v. temperature curve with a set of maximums or peaks of light intensity, which reflect the traps or groups of traps that are present.

Dating by thermoluminescence

One of the principal applications of TL is dating ancient ceramics, taking advantage of the ability of quartz, within ceramic sherds, to *trap* electrons in traps or defects in the crystal. In the production of ceramics, the clay matrix is subjected to temperatures above 700°C, which eliminates all accumulated energy in the quartz since its geological formation. From this point on, these crystals function as a *thermoluminescence clock*, since electron traps begin storing energy from radiation emitted by the radioactive elements U^{238} , Th^{232} , K^{40} , among others, which are present in the sherd itself and in the surrounding areas where it was buried. In this way, the radiation dose that the sample absorbs is proportional to the time elapsed since its last heating to high temperatures. Hence a TL date of a ceramic sherds takes into account the determination of the total radiation dose absorbed by the sherd, called the paleodose (P) and the radiation dose supplied each year by the sample and the surrounding dirt, called the mean annual dose (D). The age of the sherd is estimated from the quotient of P and D.

The laboratory process begins with the extraction of quartz from the clay matrix. A mechanical treatment reduces the ceramic fragment to dust and then it is bathed in HCl and HF to isolate clean and stripped quartz grains. After a series of washes with distilled water, the sample is screened until grains are all of a similar size, 100 microns in diameter.

Determining the paleodose P requires studying the dosimetric properties of the quartz crystal, that is, an analysis of the TL light response versus the ionizing radiation dose. The most commonly-used methods for this are called *Plateau*, Additive, and Pre-dose (M.J. Aitken, 1985). The first two make it possible to obtain the equivalent dose Q , which is the radiation dose that returns a TL signal equivalent to the natural signal of the ceramic sherd. To get to the value of paleodosis P , it is necessary to make a correction of the equivalent dose Q through the study of the phenomenon of superlinearity, different for each sample of quartz from the ceramic matrix.

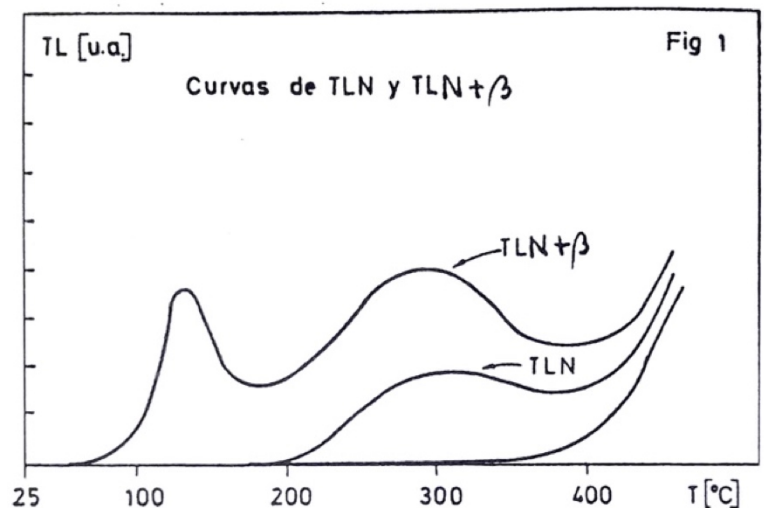
Method for calculating equivalent dose (Q)

1. *Plateau* method

The sample of quartz grains, extracted from the sherd with mechanical and chemical methods, is heated at $20^{\circ}\text{C}/\text{second}$, as light is recorded in function of temperature. This plot shows the natural thermoluminescence curve (NTC), as in figure 1. The part of the curve between room temperature and 200°C in which light emission is practically null. This is because the TL traps in this range have suffered significant electron loss while buried, that is, that have a shorter half-life than the age of the sherd. On the other hand, the TL traps that originate around 350°C have a half-life that is much longer than the age of the sherd and they have not undergone such losses. This stable range (starting at 350°C) is used to calculate the equivalent dose Q .

In another sample, similar to the one used to obtain the NTC, is subjected to a radiation dose from a calibrated radioactive source, and following a similar approach, the curve $\text{TLN}+\beta$ is obtained, as shown in figure 1.

The quotient $\text{TLN}/\text{TLN}+\beta$ is graphed against temperature, which results in a curve that, beginning at this zero, reaching a constant value at approximately 375°C called the *plateau* (figure 2). This represents the stable part



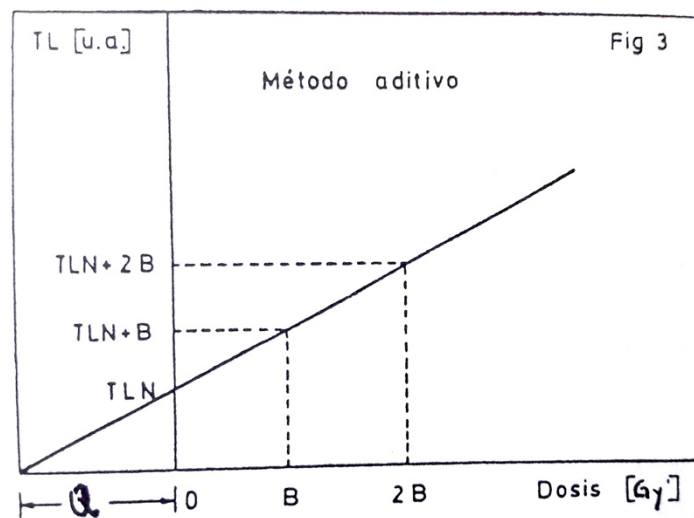
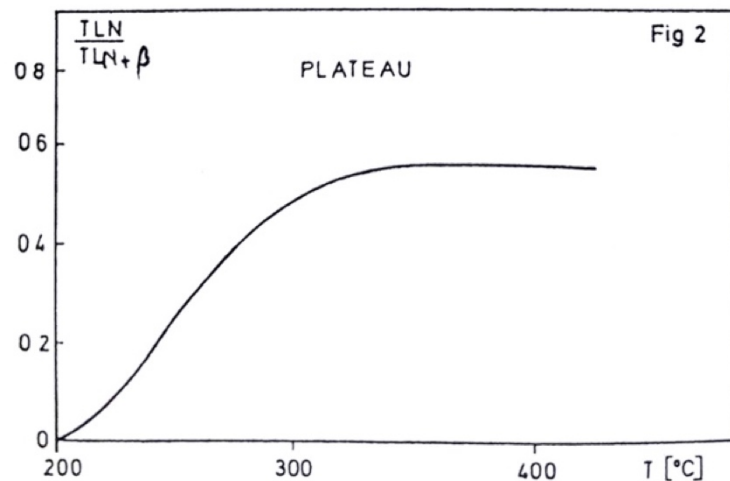
of the curve that makes it possible to determine the equivalent dose Q .

2. Additive method

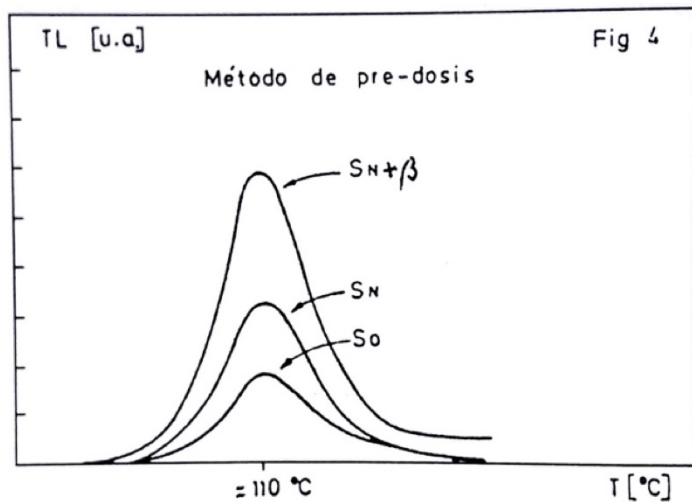
At least three identical samples are required from the sherd. With the first, the NTC is obtained; the others are subjected to an additional radioactive dose β and 2β , thereby recording $NTC+\beta$ and $NTC+2\beta$, respectively. Plotting this light emission at 375°C (or around that temperature) in function of the additional dose, a straight line is obtained and the value Q is where the line crosses the x-axis. (figure 3)

3. Pre-dose method

For this method, the high sensitivity of the trap is used, which for quartz is the 100°C signal. Even though this signal does not appear in the NTC, it *memorizes* the radioactive dose that the sherd received since its last heating, or pre-dose, modifying the sensitivity after being irradiated. For this method, the paleodose P is obtained by irradiating the sample (the quartz from the sherd) with a small test dose to obtain the S_0 signal at 110°C . After being heated to 500°C , it is irradiated again with the previous dose to return the S_N value.



The same is subjected to a dose of β Gy (the radiation dose is measured in grays or Gy; 1 Gy = 1 joule/kg) and heated to 500°C. Finally, it is irradiated at the test dose to obtain the signal $S_{N+\beta}$. The changes in sensitivity are proportional to the posterior radiation doses of each heating; this particular characteristic of quartz makes it possible to directly determine the Paleodose P. (figure 4)



Calculation of the annual dose

The radioactive dose the sherd is subjected to, beginning from its last heating, comes principally from radioactive elements present in the sample itself and the surrounding soil: U^{238} , Th^{232} , and K^{40} . These natural sources emit alpha and beta particles and gamma radiation that are responsible for the NTC. The sum of the average contributions of each one of these emitters is the annual radiation dose D that the sample is subjected to.

The calculation of D can be done with many methods. Among other methods, it is worth mentioning the determination of radioactive trace elements by neutron activation. However, the need to quantify the radioactive elements of the sherd and the surrounding soil make the dating process quite difficult. Instead, a direct calculation of D with *in situ* dosimetry can rectify this problem; high-sensitivity dosimeters buried over long periods (a few months) in the place where the sherd was found make it possible to obtain a more precise annual radiation dose than calculating radioactive trace elements.

Experimental Details

TL measurement, the basis for the dates presented in this book, were done with a model 2000 A-B Harshaw thermoluminescent analyzer. Quartz samples were extracted from ceramics

and heated from room temperature to 550°C at a rate of 12°C/second in an inert atmosphere created with a flow extra pure nitrogen oxide at 4 L/minute. The artificial irradiations, to measure the paleodose, were done with a radioactive source of ^{90}Sr (10 mCi, nominal) that delivers a dose of 1.2 Gy/minute.

The annual radiation dose D was calculated with thermoluminescence dosimetry (A. Deza et al., 1986). The average dose, in both the field and each of the sherds, was measured using $\text{CaSO}_4:\text{Dy}$ dosimeters, which are preferred over other crystals because of reduced *fading* (loss of information) and energy independence.

Error estimates were made using the method suggested by M.J. Aitken (1976), assuming zero for all 3σ uncertainties (lithic content of the soil) and 7σ (radiation emission).

Advantages and disadvantages of the method

TL dating has advantages over other methods, especially ^{14}C . Compared to this method, TL assembly is simpler and has a much lower cost. Additionally, sample preparation does not require the extremely precise chemical treatments required for radiocarbon counting. Within certain ranges, TL response increase over time, the opposite of what happens with ^{14}C .

In terms of the disadvantages of TL, one that can be mentioned is that it is only possible to date archaeological samples that have crystalline inclusions, such as quartz in the case of ceramics: hence TL cannot date metal objects or organic samples.

The problem with the *archaeological zero* is another limitation that must be carefully assessed. In effect, as mentioned, this corresponds to the moment of ceramic production, that is, the last heating to high temperatures (above 550°C). However, imported ceramics and those passed down from generation to generation add uncertainty to the reliability of TL dates. In the end, archaeologists are not after the date of ceramic production, which is what this method offers, but the date of when the sherd was introduced to the excavation context. For this reason, it is recommended that the sample is, whenever possible, from an everyday domestic ceramic vessel that also has evidence of being heated to high temperatures, whether at the time of production or in a hearth as a cooking vessel. Heating to high temperatures is of enormous

importance, since low temperatures in the original firing can result in an early date for a late artifact.

Bibliographic references

Aitken, M.J. **Thermoluminescence Dating**. London, Academic Press. 1985.

Aitken, M.J. *Thermoluminescent age evaluation and assessment of error limit: revised system*.

Archaeometry 18. 1979. Pp233-238.

Daniels, F, Boyd, C.A and Sanders, D.F. Thermoluminescence as a research tool. **Science** 177.

1953. Pp. 343-349.

Deza, A., Román, A. La dosimetría termoluminiscente en arqueología. **Revista Chungara**. N°16

16-17. 1986. Pp. 403-407.

Supplementary Material 2. OxCal code for Bayesian models of dates from the Azapa Valley, Chile, and the Inca occupation of northern Mendoza.

```
Plot()
{
  Curve("SHCal20", "SHCal20.14c");
  Sequence()
  {
    Boundary("Start Cabuza TL");
    KDE_Plot("Cabuza TL")
    {
      C_Date("UCTL-161, Az-143, Tomb 6", 755, 120);
      C_Date("UCTL-600, Az-13, Tomb J4/1", 775, 120);
      C_Date("UCTL-588, Az-3, Tomb DJ8", 805, 100);
      C_Date("UCTL-581, Az-3, Tomb J10/2b", 860, 80);
      C_Date("UCTL-594, Az-3, Tomb Q4/3", 865, 80);
      C_Date("UCTL-165, Az-141, Tomb 24", 890, 100);
      C_Date("UCTL-592, Az-3, Tomb K5/1", 890, 100);
      C_Date("UCTL-593, Az-3, Tomb M10/2", 935, 80);
      C_Date("UCTL-598, Az-3, Tomb DJ23", 940, 50);
      C_Date("UCTL-590, Az-3, Tomb M10/1", 970, 80);
      C_Date("UCTL-158, Az-6, Tomb 103", 1020, 100);
      C_Date("UCTL-595, Az-3, Tomb J10/1", 1070, 90);
      C_Date("UCTL-157, Az-6, Tomb 24", 1070, 120);
      C_Date("UCTL-102, Ex asentamiento Manuel Rodríguez, looted tomb", 1070, 50);
      C_Date("UCTL-648, Az-103, Surface find", 1120, 90);
      C_Date("UCTL-651, Az-3, Tomb M9/1", 1195, 80);
      C_Date("UCTL-647, Az-103, Surface find", 1225, 70);
    };
    Boundary("End Cabuza TL");
  };
  Sequence()
  {
    Boundary("Start Cabuza 14C");
    KDE_Plot("Cabuza 14C")
    {
      R_Date("I-13780, Az-141, Tomb 24", 930, 80);
      R_Date("Hela-3184, Az-6, Tomb 102", 924, 28);
      R_Date("Hela-3185, Az-6, Tomb 121", 877, 29);
      R_Date("Hela-3182, Az-6, Tomb 34", 881, 28);
      R_Date("Hela-3180, Az-6, Tomb 6", 926, 29);
      R_Date("Hela-3183, Az-6, Tomb 66", 890, 28);
      R_Date("Beta-77222, Az-71, Tomb 147", 830, 50);
      R_Date("Hela-3332, Az-71a, Tomb 132", 898, 34);
    };
    Boundary("End Cabuza 14C");
  };
  Sequence()
  {
    Boundary("Start Maytas-Chiribaya TL");
    KDE_Plot("Maytas-Chiribaya TL")
    {
      C_Date("UCTL-584, Az-3, Tomb U10/1", 840, 110);
      C_Date("UCTL-586, Az-79, Tomb F8/1a", 890, 100);
      C_Date("UCTL-597, Az-3, Tomb M10/3", 950, 110);
      C_Date("UCTL-166, Az-75, Tomb 116", 995, 80);
      C_Date("UCTL-653, Az-105, Tomb T1", 1015, 80);
    };
  };
}
```

```

C_Date("UCTL-589, Az-3, Tomb T11/1",1120,90);
C_Date("UCTL-585, Az-8, Tomb M2/1",1160,80);
C_Date("UCTL-583, Az-75, Tomb T101",1215,60);
C_Date("UCTL-601, Az-105, Tomb T5",1260,70);
C_Date("UCTL-591, Az-3, Tomb N12/2",1260,60);
C_Date("UCTL-107, Ex asentamiento Manuel Rodríguez, Looted tomb",1260,100);
C_Date("UCTL-604, Az-8, Tomb Ñ2/1",1290,70);
};
Boundary("End Maytas-Chiribaya TL");
};
Sequence()
{
Boundary("Start Maytas-Chiribaya 14C");
KDE_Plot("Maytas-Chiribaya 14C")
{
R_Date("Beta-78628, Az-140, Tomb 28",560,50);
R_Date("GAK-5817, Az-6, Tomb 127",1220,80);
R_Date("I-11622, Az-6, Tomb 141",715,130);
R_Date("I-11625, Az-6, Tomb 141",910,145);
R_Date("Hela-3142, Az-6, Tomb 163",918,29);
R_Date("I-11621, Az-71",765,75);
R_Date("Beta-78958, Az-71, Tomb 174",850,50);
R_Date("I-11641, Az-71, Tomb 480",695,75);
R_Date("Hela-3329, Az-71a, Tomb 24",759,35);
R_Date("I-11624, PLM-9, Tomb 24",1055,80);
};
Boundary("End Maytas-Chiribaya 14C");
};
Sequence()
{
Boundary("Start San Miguel TL");
KDE_Plot("San Miguel TL")
{
C_Date("UCTL-603, Az-8, Tomb S9/2",990,80);
C_Date("UCTL-587, Az-8, Tomb S9/3",1030,90);
C_Date("UCTL-105, Ex asentamiento Manuel Rodríguez, Looted tomb",1030,50);
C_Date("UCTL-110, Poblado de Sabaipugro, Enclosure 24",1190,90);
};
Boundary("End San Miguel TL");
};
Sequence()
{
Boundary("Start San Miguel 14C");
KDE_Plot("San Miguel 14C")
{
R_Date("Beta-78627, Az-140, Tomb 6",450,50);
R_Date("Hela-3143, Az-6, Tomb 202",636,30);
R_Date("Hela-3331, Az-71a, Tomb 72",563,35);
R_Date("UCLA-1294B, Az-8, Tomb M-10",280,80);
R_Date("UCLA-1294C, Az-8, Tomb M-27",580,80);
R_Date("UCLA-1294D, Az-8, Tomb M-42",810,80);
R_Date("UCLA-1294A, Az-8, Tomb M-45",680,80);
R_Date("I-10861, PLM-9, Tomb 14",775,80);
R_Date("Beta-78635, PLM-9, Tomb 18",640,50);
R_Date("Hela-3181, Az-6, Tomb 7",782,28);
};
Boundary("End San Miguel 14C");
};
};
};

```

```

Plot()
{
Curve("SHCal20", "SHCal20.14c");
Sequence()
{
Boundary("Start Inca 14C");
KDE_Plot("Inca 14C")
{
R_Date("Laguna del Diamante-13, LP-3539, Ext. 5", 420,40);
R_Date("Laguna del Diamante-4, LP-3658, Ext. 5", 490,40);
R_Date("Alero Ernesto, Beta-162400", 460,60);
R_Date("El Chacay, LP-3598", 530,40);
R_Date("Las Cuevas 2, LP-3602", 440,40);
R_Date("Risco de Los Indios, AA-102653, nivel 10", 478,38);
R_Date("Risco de Los Indios, UGAMS-13578, nivel 7", 500,20);
R_Date("Risco de Los Indios, UGAMS 13579, nivel 6", 480,20);
R_Date("Ciénaga de Yalguaraz, UZ-2525/ETH-5318", 485, 60);
R_Date("Ciénaga de Yalguaraz, UZ-2526/ETH-5319", 540, 55);
R_Date("Ciénaga de Yalguaraz, GaK-7312", 390, 90);
R_Date("Ciénaga de Yalguaraz, UZ-2527/ETH-5320", 420, 60);
R_Date("Tambillos, Beta-25221", 770, 50);
R_Date("Tambillos, Beta-26283", 410, 70);
R_Date("Tambillos, I-16637", 290, 130);
R_Date("Tambillos, I-16908", 300, 80);
R_Date("Tambillos, I-16907", 310, 80);
R_Date("Ranchillos, Beta-69934", 640, 50);
R_Date("Ranchillos, Beta-69933", 430, 50);
R_Date("Ranchillos, I-17002", 290, 80);
R_Date("Ranchillos, I-17003", 220, 80);
R_Date("Ranchillos, I-17004", 300, 80);
R_Date("Tambillitos, Beta-88786", 540, 100);
R_Date("Tambillitos, Beta-88787", 460, 80);
R_Date("Agua Amarga, Beta-261727", 450, 50);
R_Combine("Aconcagua")
{
R_Date("GX-19991", 370, 70);
R_Date("Beta-88785", 480, 40);
};
R_Date("Cerro Penitentes, Beta-98941", 550, 50);
R_Date("Potrero Las Colonias, AA-66564", 569, 38);
R_Date("Agua de la Cueva, AC-1563", 470, 80);
R_Date("Odisa, AA-90284", 529, 42);
Span("Span Inca 14C");
};
Boundary("End Inca 14C");
};
};

```

```

Plot()
{
Sequence()
{
Boundary("Start Inca TL");
KDE_Plot()
{
C_Date("Tambillos, UCTL-301", AD(1350), 60);
C_Date("Tambillos, UCTL-302", AD(1630), 40);
C_Date("Tambillos, UCTL-303", AD(1510), 50);

```

```
C_Date("Tambillos, UCTL-304", AD(1355), 70);
C_Date("Tambillos, UCTL-306", AD(1510), 50);
C_Date("Ciénaga de Yalguaraz, UCTL-315", AD(1440), 60);
C_Date("Ranchillos, UCTL-317", AD(1620), 30);
C_Date("Ciénaga de Yalguaraz, UCTL-321", AD(1540), 40);
C_Date("Ciénaga de Yalguaraz, UCTL-322", AD(1520), 40);
C_Date("Tambillitos, UCTL-323", AD(1555), 45);
C_Date("Ranchillos, UCTL-337", AD(1595), 45);
C_Date("Ranchillos, UCTL-488", AD(1490), 50);
C_Date("Ranchillos, UCTL-499", AD(1480), 50);
C_Date("Ranchillos, UCTL-785", AD(1480), 50);
C_Date("Ranchillos, UCTL-786", AD(1555), 45);
C_Date("Tambillitos, UCTL-787", AD(1440), 60);
C_Date("La Chanchería, UCTL-2093", AD(1505), 50);
C_Date("La Chanchería, UCTL-2376", AD(1570), 40);
C_Date("Agua Amarga, UCTL 1725c",AD(1432),55);
C_Date("Agua Amarga, UCTL 1724c",AD(1608),40);
C_Date("Agua Amarga, UCTL 1726c",AD(1563),48);
Span("Inca TL");
};
Boundary("End Inca TL");
Before("Sites in ruins", AD(1595));
};
};
```

LUMINESCENCE ANALYSIS OF CERAMICS FROM ARGENTINA

7 March 2019

James K. Feathers
Luminescence Dating Laboratory
University of Washington
Seattle, WA 98195-3412
Email: jimf@uw.edu

This report presents the results of luminescence analysis of six ceramic samples from Mendoza province, Argentina. The samples were submitted by Erik Marsh of the National Research Council-Argentina. Dates on five ceramics were requested but a sixth ceramic was submitted as a backup for one ceramic that was rather small. The laboratory ended up processing all six. Similar samples were previously processed by a luminescence laboratory in Santiago, Chile, but these dates were all reported at about 500 years, which did not agree with other information. Provenience data on the ceramics are given in Table 1. Laboratory procedures are given in the appendix.

Table 1. Sample information

UW Lab #	Sherd #	Site	Site type	Context	Burial depth (cm)
UW3754	1	Agua de la Cueva	Cave	Organic matrix with high density of artifacts	115-120
UW3755	2	Agua de la Cueva	Cave	Organic matrix with high density of artifacts	115-120
UW3756	3	Las Cuevas 2	Cave		30-35
UW3757	4	El Manzana Histórico 2	Open air	Pit house floor	20-25
UW3758	5	Barrancas 61	Open air	Pit house floor	10-15
UW3759	6	Paso de Parmillos	Cave	Organic matrix with high density of artifacts	62-64

Dose rate

The dose rate was measured on each ceramic as described in the appendix, but no associated sediment samples were available to determine the external gamma dose rate. Ages were calculated both assuming the sediment radioactivity was the same as the sherds and assuming concentrations of 0.5% K, 6 ppm Th and 2 ppm U. This provides a reasonable range for the external dose rate. Concentrations of radionuclides are given in Table 2.

Dose rates on the ceramics were mainly determined using alpha counting and flame photometry. The beta dose rate calculated from these measurements was compared with the beta dose rate measured directly by beta counting. Table 2 compares the beta dose rate calculated in these two ways. These differ significantly only for UW3755. The problem, I believe, is a severe under-estimation of the K content for this sample. UW3754, from the same context, had similar U and Th contents, but much higher K content. An assumed K content of 2% for UW3755 is similar to the value measured for UW3754 and brings the two measures of beta dose rate into agreement.

Moisture content was estimated as 30±30 % of the saturated value for the ceramics, reflecting the arid environment (and cave setting for some samples), and 6 ± 3 % for the sediments. Cosmic dose rate was determined from Prescott and Hutton (1994), using the latitude, longitude and altitude of the sites and burial depths of the sherds. For the cave settings, adjustment for the over-burden was

estimated by dividing the calculated cosmic dose rate by 4 for UW3756 and by 3 for the others, reflecting the configuration of the opening and the distance back from the dripline. The cosmic dose rate makes up a small portion of the total dose rate, so obtaining further precision is not critical. Table 3 gives the total dose rates.

Table 2. Radionuclide concentrations

Sample	²³⁸ U (ppm)	²³³ Th (ppm)	K (%)	Beta dose rate (Gy/ka)	
				β-counting	α-counting/flame photometry
UW3754	3.83±0.26	10.42±1.37	2.34±0.25	2.90±0.24	2.76±0.24
UW3755	3.45±0.24	10.03±1.23	0.66±0.07	2.16±0.18	1.33±0.08
UW3756	2.07±0.17	8.53±1.17	2.41±0.26	2.69±0.24	2.51±0.22
UW3757	2.25±0.16	4.78±0.88	1.01±0.10	1.44±0.12	1.29±0.09
UW3758	2.25±0.20	11.72±1.42	2.01±0.21	2.39±0.20	2.30±0.18
UW3759	2.69±0.20	8.94±1.25	2.38±0.25	2.72±0.28	2.60±0.21

Table 3. Dose rates (Gy/ka)*

Sample	alpha	beta	gamma	cosmic	total
UW3754	0.70±0.11	2.57±0.27	1.41±0.09	0.07±0.01	4.75±0.30
UW3755	1.08±0.31	2.31±0.19	1.27±0.08	0.07±0.01	4.73±0.37
UW3756	0.42±0.04	2.35±0.25	1.16±0.08	0.07±0.01	4.01±0.27
UW3757	0.80±0.06	1.25±0.10	0.69±0.05	0.26±0.05	2.99±0.14
UW3758	0.60±0.05	2.17±0.21	1.13±0.12	0.25±0.05	4.15±0.25
UW3759	0.58±0.05	2.49±0.23	1.24±0.09	0.08±0.02	4.39±0.25

* Dose rates for ceramics are calculated for OSL, assuming the sediment has the same radioactivity as the ceramic and assuming a K content of 1.98 for UW3755. Dose rates will usually be higher for TL and IRSL due to higher b-values. Also the beta dose rate is lower than that given in Table 2 due to moisture correction.

Equivalent Dose

Equivalent dose was measured for TL, OSL and IRSL as described in the appendix. The TL data for UW3755 were too poor, because of small sample size, for an equivalent dose to be determined. For the other samples, the TL plateaus were broad. There was no sensitivity change between first and second glowouts. TL anomalous fading was evident in all samples but a fading correction produced finite values only for UW3757, UW3758, and UW3759.

Table 4. TL parameters

Sample	Plateau (°C)	1 st /2 nd ratio*	fit	Fading g-value**
UW3754	250-340	1.0	quadratic	19.9±9.78
UW3756	260-390	1.0	linear	30.7±7.72
UW3757	250-400	1.0	linear	8.78±0.88
UW3758	260-360	1.0	Quadratic	9.52±2.21
UW3759	270-380	1.0	linear	5.67±4.61

*Refers to slope ratio between the first and second glow growth curves. A glow refers to luminescence as a function of temperature; a second, or regeneration glow comes after heating to 450°C.

** A g-value is a rate of anomalous fading, measured as percent of signal loss per decade, where a decade is a power of 10. Any value over about 14 results in an infinite age correction, implying the fading rate has probably changed through time.

OSL/IRSL was measured on 6-9 aliquots per sample (Table 5), but some aliquots were rejected because of poor data. Scatter was less than 20% for all samples. An IRSL signal could be measured on all samples, but the IRSL signal was from 5 to 25 times less intense than the OSL signal. IRSL stems from feldspars, which are prone to anomalous fading. A relatively strong IRSL signal may suggest the OSL signal partly stems from feldspars and therefore may fade, while a weak IRSL suggests the OSL is dominated by quartz, although IRSL is generally weaker than OSL in ceramics because heat reduces the IRSL intensity while increasing the OSL intensity. Another measure of feldspar contribution is the size of the OSL b-value. The b-value is a measure of alpha luminescence efficiency, and is usually less than 0.7 for quartz and a higher value for feldspar. For these samples the OSL b-value was in the range of quartz for all samples but UW3755 and UW3757. It is possible the OSL signal in these two samples partly stems from feldspars and thus the signal may fade some.

As a test of the SAR procedures, a dose recovery test was performed. The recovered dose was within 2-sigma of the administered dose for all samples, but UW3756, where it was close, and UW3757, where the recovered dose was much higher. It is uncertain why this was the case for UW3757. Equivalent dose and b-values are given in Table 6.

Table 5. OSL/IRSL data

Sample	# aliquots*		OSL Over-dispersion (%)	Dose Recovery (OSL)	
	OSL	IRSL		Given Dose (sβ)	Recovered Dose (sβ)
UW3754	5	3	13.2±4.5	20	21.1±0.92
UW3755	5	6	18.1±6.7	50	47.0±3.20
UW3756	6	5	0	20	25.1±1.83
UW3757	5	6	7.0±3.7	20	51.4±2.9
UW3758	9	8	8.1±2.3	40	37.9±2.0
UW3759	9	4	3.3±2.3	40	35.7±3.0

* Denotes number of aliquots with measurable signals.

Table 6. Equivalent dose and b-value – fine grains

Sample	Equivalent Dose (Gy)			b-value (Gy μm ²)		
	TL	IRSL	OSL	TL	IRSL	OSL
UW3754	2.16±0.17	5.49±0.94	4.84±0.30	1.81±0.37	1.88±0.42	0.65±0.08
UW3755		4.94±0.70	3.38±0.30		0.90±0.62	1.04±0.27
UW3756	47.8±14.3	8.06±0.74	6.23±0.14	1.94±0.47	1.09±0.30	0.60±0.03
UW3757	2.38±0.32	3.25±0.18	4.48±0.18	3.22±0.49	1.18±0.09	1.34±0.06
UW3758	9.66±0.68	6.51±0.73	5.40±0.16	1.47±0.31	1.84±0.42	0.67±0.02
UW3759	3.55±0.32	4.32±0.99	4.72±0.90	1.02±0.13		0.68±0.04

Ages

Table 7 gives the derived ages for each sample. For UW3754, the OSL and the IRSL ages were in statistical agreement. The TL age was younger probably because of fading, but the fading rate was too high to produce a finite correction. For UW3755, the IRSL age was actually older than the OSL age (contrary to expectations), but they were in agreement at 2σ . For UW3756, the OSL and IRSL ages were in statistical agreement, but the TL age was much older, perhaps suggesting that the TL signal was not completely reset. For UW3757, the OSL signal produced the oldest age. TL and IRSL probably suffered from anomalous fading, but the TL correction was based on only two points and not reliable. Because of the high OSL b-value, it is possible the age for this sample is slightly underestimated. For UW3758, the OSL and IRSL signals were in statistical agreement. The TL was older, again perhaps because of poor resetting. For UW3759, the TL corrected for fading and the OSL were in statistical agreement, but the error on the TL was quite high, so only the OSL is listed in Table 7. An IRSL age could not be obtained because of weak signal when trying to compute the b-value.

Using the low assumed external dose rate produced ages about 100-200 years older than using the ceramic radioactivity for the external dose rate, but the differences for all samples are with 1σ errors. The difference for UW3757 is small because the radioactivity of that sample was comparatively low.

Surprisingly, the IRSL signal produced an age in agreement with the OSL signal for most samples. This suggests that anomalous fading is not a significant issue for these samples, although the OSL age for UW3757 may still be a slight underestimation. The IRSL age was significantly younger for this sample, the only sample where this was the case. The ages of the two sherds from the same context, UW3754 and UW3755, are significantly different, but it is a possibility that the OSL age for UW3755 is also an underestimation, because of the high OSL b-value. On the other hand, the IRSL signal did not seem to suffer from fading in this sample, so it is not likely that the OSL signal did.

The estimated ages for all of the samples are older than the results from the Santiago lab. The reason for this discrepancy is not known. However, the Santiago lab only used the TL signal, which in our analysis was of variable quality and produced useful data only for UW3759 (although with high error terms, $\sim 30\%$).

Table 7. Ages

Sample	Age (ka)*		% error		Basis for age	Calendar date (years AD)	
	High** external dose rate	Low** external dose rate	High** external dose rate	Low** external dose rate		High** external dose rate	Low** external dose rate
UW3754	0.99±0.08	1.16±0.10	8.5	9.0	OSL/IRSL	1020 ± 80	860 ± 100
UW3755	0.76±0.08	0.87±0.10	10.7	11.3	OSL/IRSL	1260 ± 80	1150 ± 100
UW3756	1.62±0.11	1.84±0.13	6.7	7.1	OSL/IRSL	400 ± 110	180 ± 130
UW3757	1.51±0.10	1.54±0.11	6.9	6.8	OSL	510 ± 100	480 ± 110
UW3758	1.29±0.09	1.46±0.10	6.6	6.8	OSL/IRSL	730 ± 80	560 ± 100
UW3759	1.08±0.07	1.23±0.09	6.7	7.2	OSL	940 ± 70	780 ± 90

* The base year for ka is 2018.

** High external dose rate refers to use of the ceramic radioactivity for the external dose rate. Low external dose rate uses sediment radioactivity based on 0.5% K, 6 ppm Th and 2 ppm U.

Appendix:

Procedures for Thermoluminescence Analysis of Pottery

Sample preparation -- fine grain

The sherd is broken to expose a fresh profile. Material is drilled from the center of the cross-section, more than 2 mm from either surface, using a tungsten carbide drill tip. The material retrieved is ground gently by an agate mortar and pestle, treated with HCl, and then settled in acetone for 2 and 20 minutes to separate the 1-8 μm fraction. This is settled onto a maximum of 72 stainless steel discs.

Glow-outs

Thermoluminescence is measured by a Daybreak reader using a 9635Q photomultiplier with a Corning 7-59 blue filter, in N_2 atmosphere at 1°C/s to 450°C . A preheat of 240°C with no hold time precedes each measurement. Artificial irradiation is given with a ^{241}Am alpha source and a ^{90}Sr beta source, the latter calibrated against a ^{137}Cs gamma source. Discs are stored at room temperature for at least one week after irradiation before glow out. Data are processed by Daybreak TLApplic software.

Fading test

Several discs are used to test for anomalous fading. The natural luminescence is first measured by heating to 450°C . The discs are then given an equal alpha irradiation and stored at room temperature for varied times: 10 min, 2 hours, 1 day, 1 week and 8 weeks. The irradiations are staggered in time so that all of the second glows are performed on the same day. The second glows are normalized by the natural signal and then compared to determine any loss of signal with time (on a log scale). If the sample shows fading and the signal versus time values can be reasonably fit to a logarithmic function, an attempt is made to correct the age following procedures recommended by Huntley and Lamothé (2001). The fading rate is calculated as the g-value, which is given in percent per decade, where decade represents a power of 10.

Equivalent dose

The equivalent dose is determined by a combination additive dose and regeneration (Aitken 1985). Additive dose involves administering incremental doses to natural material. A growth curve plotting dose against luminescence can be extrapolated to the dose axis to estimate an equivalent dose, but for pottery this estimate is usually inaccurate because of errors in extrapolation due to nonlinearity. Regeneration involves zeroing natural material by heating to 450°C and then rebuilding a growth curve with incremental doses. The problem here is sensitivity change caused by the heating. By constructing both curves, the regeneration curve can be used to define the extrapolated area and can be corrected for sensitivity change by comparing it with the additive dose curve. This works where the shapes of the curves differ only in scale (i.e., the sensitivity change is independent of dose). The curves are combined using the "Australian slide" method in a program developed by David Huntley of Simon Fraser University (Prescott et al. 1993). The equivalent dose is taken as the horizontal distance between the two curves after a scale adjustment for sensitivity change. Where the growth curves are not linear, they are fit to quadratic functions. Dose increments (usually five) are determined so that the maximum additive dose results in a signal about three times that of the natural and the maximum regeneration dose about five times the natural.

A plateau region is determined by calculating the equivalent dose at temperature increments between 240° and 450°C and determining over which temperature range the values do not differ significantly. This plateau region is compared with a similar one constructed for the b-value (alpha efficiency), and the overlap defines the integrated range for final analysis.

Alpha effectiveness

Alpha efficiency is determined by comparing additive dose curves using alpha and beta irradiations. The slide program is also used in this regard, taking the scale factor (which is the ratio of the two slopes) as the b-value (Aitken 1985).

Radioactivity

Radioactivity is measured by alpha counting in conjunction with atomic emission for ⁴⁰K. Samples for alpha counting are crushed in a mill to flour consistency, packed into plexiglass containers with ZnS:Ag screens, and sealed for one month before counting. The pairs technique is used to separate the U and Th decay series. For atomic emission measurements, samples are dissolved in HF and other acids and analyzed by a Jenway flame photometer. K concentrations for each sample are determined by bracketing between standards of known concentration. Conversion to ⁴⁰K is by natural atomic abundance. Radioactivity is also measured, as a check, by beta counting, using a Risø low level beta GM multiscaler system. About 0.5 g of crushed sample is placed on each of four plastic sample holders. All are counted for 24 hours. The average is converted to dose rate following Bøtter-Jensen and Mejdahl (1988) and compared with the beta dose rate calculated from the alpha counting and flame photometer results. Associated sediments were not available for dose rate analysis. Cosmic radiation is determined after Prescott and Hutton (1994). Radioactivity concentrations are translated into dose rates following Guérin et al. (2011).

Moisture Contents

Water absorption values for the sherds are determined by comparing the saturated and dried weights. For temperate climates, moisture in the pottery is taken to be 80 ± 20 percent of total absorption, unless otherwise indicated by the archaeologist. Again for temperate climates, soil moisture contents are taken from typical moisture retention quantities for different textured soils (Brady 1974: 196), unless otherwise measured. For drier climates, moisture values are determined in consultation with the archaeologist.

Procedures for Optically Stimulated or Infrared Stimulated Luminescence of Fine-grained pottery.

Optically stimulated luminescence (OSL) and infrared stimulated luminescence (IRSL) on fine-grain (1-8µm) pottery samples are carried out on single aliquots following procedures adapted from Banerjee et al. (2001) and Roberts and Wintle (2001). Equivalent dose is determined by the single-aliquot regenerative dose (SAR) method (Murray and Wintle 2000).

The SAR method measures the natural signal and the signal from a series of regeneration doses on a single aliquot. The method uses a small test dose to monitor and correct for sensitivity changes brought about by preheating, irradiation or light stimulation. SAR consists of the following steps: 1) preheat, 2) measurement of natural signal (OSL or IRSL), L(1), 3) test dose, 4) cut heat, 5) measurement of test dose signal, T(1), 6) regeneration dose, 7) preheat, 8) measurement of signal from regeneration,

L(2), 9) test dose, 10) cut heat, 11) measurement of test dose signal, T(2), 12) repeat of steps 6 through 11 for various regeneration doses. A growth curve is constructed from the $L(i)/T(i)$ ratios and the equivalent dose is found by interpolation of $L(1)/T(1)$. Usually a zero regeneration dose and a repeated regeneration dose are employed to insure the procedure is working properly. For fine-grained ceramics, a preheat of 240°C for 10s, a test dose of 3.1 Gy, and a cut heat of 200°C are currently being used, although these parameters may be modified from sample to sample.

The luminescence, $L(i)$ and $T(i)$, is measured on a Risø TL-DA-15 automated reader by a succession of two stimulations: first 100 s at 60°C of IRSL (880nm diodes), and then 100s at 125°C of OSL (470nm diodes). Detection is through 7.5mm of Hoya U340 (ultra-violet) filters. The two stimulations are used to construct IRSL and OSL growth curves, so that two estimations of equivalent dose are available. Anomalous fading usually involves feldspars and only feldspars are sensitive to IRSL stimulation. The rationale for the IRSL stimulation is to remove most of the feldspar signal, so that the subsequent OSL (post IR blue) signal is free from anomalous fading. However, feldspar is also sensitive to blue light (470nm), and it is possible that IRSL does not remove all the feldspar signal. Some preliminary tests in our laboratory have suggested that the OSL signal does not suffer from fading, but this may be sample specific. The procedure is still undergoing study.

A dose recovery test is performed by first zeroing the sample by exposure to light and then administering a known dose. The SAR protocol is then applied to see if the known dose can be obtained.

Alpha efficiency will surely differ among IRSL, OSL and TL on fine-grained materials. It does differ between coarse-grained feldspar and quartz (Aitken 1985). Research is currently underway in the laboratory to determine how much b-value varies according to stimulation method. Results from several samples from different geographic locations show that OSL b-value is less variable and centers around 0.5. IRSL b-value is more variable and is higher than that for OSL. TL b-value tends to fall between the OSL and IRSL values. We currently are measuring the b-value for IRSL and OSL by giving an alpha dose to aliquots whose luminescence have been drained by exposure to light. An equivalent dose is determined by SAR using beta irradiation, and the beta/alpha equivalent dose ratio is taken as the b-value. A high OSL b-value is indicative that feldspars might be contributing to the signal and thus subject to anomalous fading.

Age and error terms

The age and error for both OSL and TL are calculated by a laboratory constructed spreadsheet, based on Aitken (1985). All error terms are reported at 1-sigma.

References

Adamiec, G., and Aitken, M. J., 1998, Dose rate conversion factors: update. *Ancient TL* 16:37-50.

Aitken, M. J., 1985, *Thermoluminescence Dating*, Academic Press, London.

Banerjee, D., Murray, A. S., Bøtter-Jensen, L., and Lang, A., 2001, Equivalent dose estimation using a single aliquot of polymineral fine grains. *Radiation Measurements* 33:73-93.

- Bøtter-Jensen, L, and Mejdahl, V., 1988, Assessment of beta dose-rate using a GM multi-counter system. *Nuclear Tracks and Radiation Measurements* 14:187-191.
- Brady, N. C., 1974, *The Nature and Properties of Soils*, Macmillan, New York.
- Guérin, G., Mercier, N., and Adamiec, G., 2011, Dose-rate conversion factors: update. *Ancient TL* 29:5-8.
- Huntley, D. J., and Lamothe, M., 2001, Ubiquity of anomalous fading in K-feldspars, and measurement and correction for it in optical dating. *Canadian Journal of Earth Sciences* 38:1093-1106.
- Mejdahl, V., 1983, Feldspar inclusion dating of ceramics and burnt stones. *PACT* 9:351-364.
- Murray, A. S., and Wintle, A. G., 2000, Luminescence dating of quartz using an improved single-aliquot regenerative-dose protocol. *Radiation Measurements* 32:57-73.
- Prescott, J. R., Huntley, D. J., and Hutton, J. T., 1993, Estimation of equivalent dose in thermoluminescence dating – the *Australian slide* method. *Ancient TL* 11:1-5.
- Prescott, J. R., and Hutton, J. T., 1994, Cosmic ray contributions to dose rates for luminescence and ESR dating: large depths and long time durations. *Radiation Measurements* 23:497-500.
- Roberts, H. M., and Wintle, A. G., 2001, Equivalent dose determinations for polymineralic fine-grains using the SAR protocol: application to a Holocene sequence of the Chinese Loess Plateau. *Quaternary Science Reviews* 20:859-863.

Supplementary Material 4: photos of the sherds and sherd profiles (40× magnification) from the pilot study.

ALC
B-24-NE
MP881

ALC 199
A-50
Ext. 24.
delgado
de los peltidos
(252)

Las Cuevas
siglo. 170
Ext. 7 andeo 1
LCSZ
(TL)

MANZANO HISTÓRICO 2
Mapa 17 cuad.
Ext. 5 zona 1 (Z1)

BG1
Cvad. B
Ext. 3.

PARAMILLOS
CUAD 2
LOCUS 22
~62-64 cm prof.



①

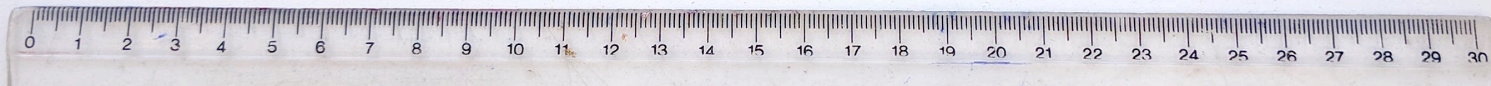
②

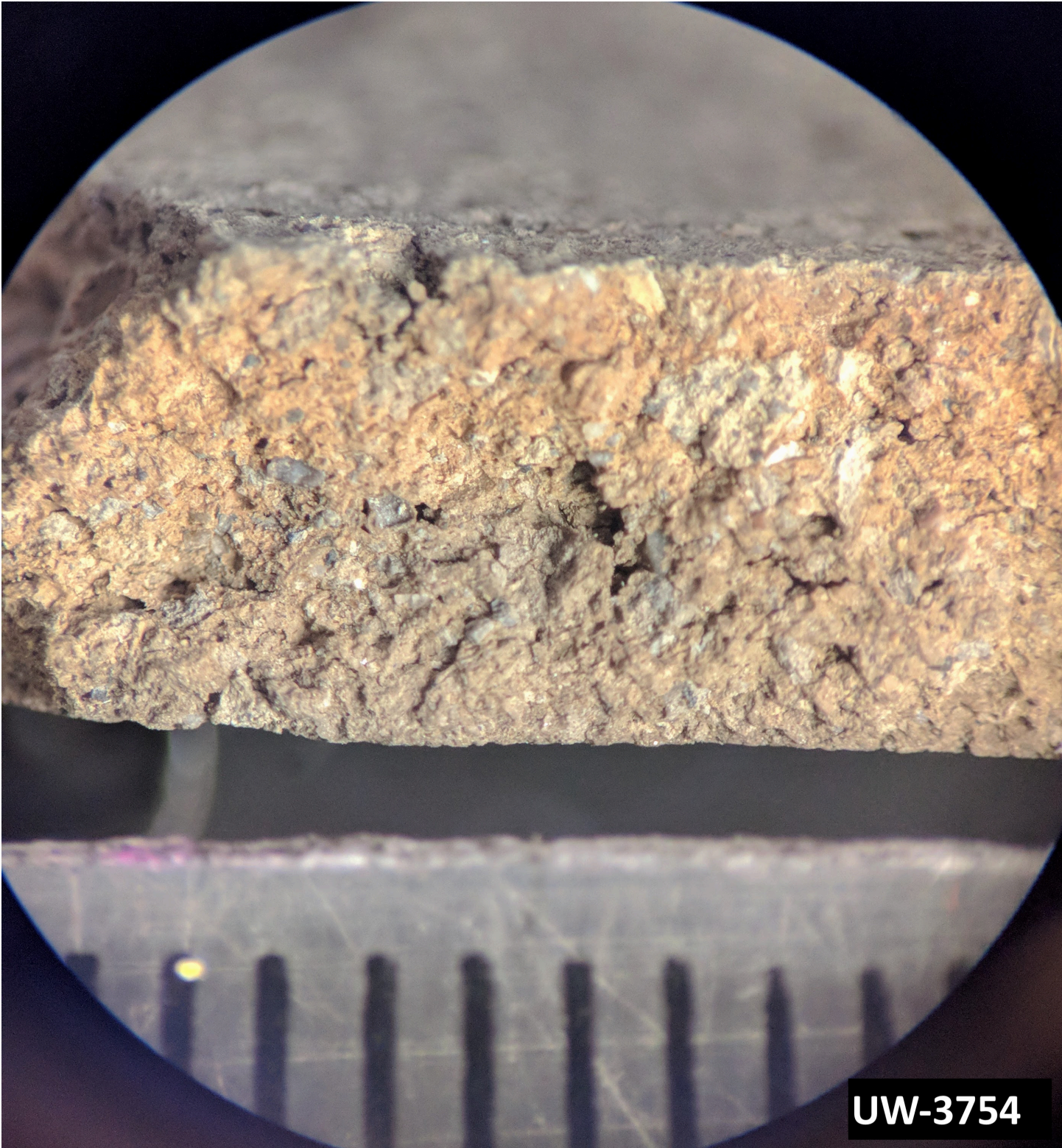
③

④

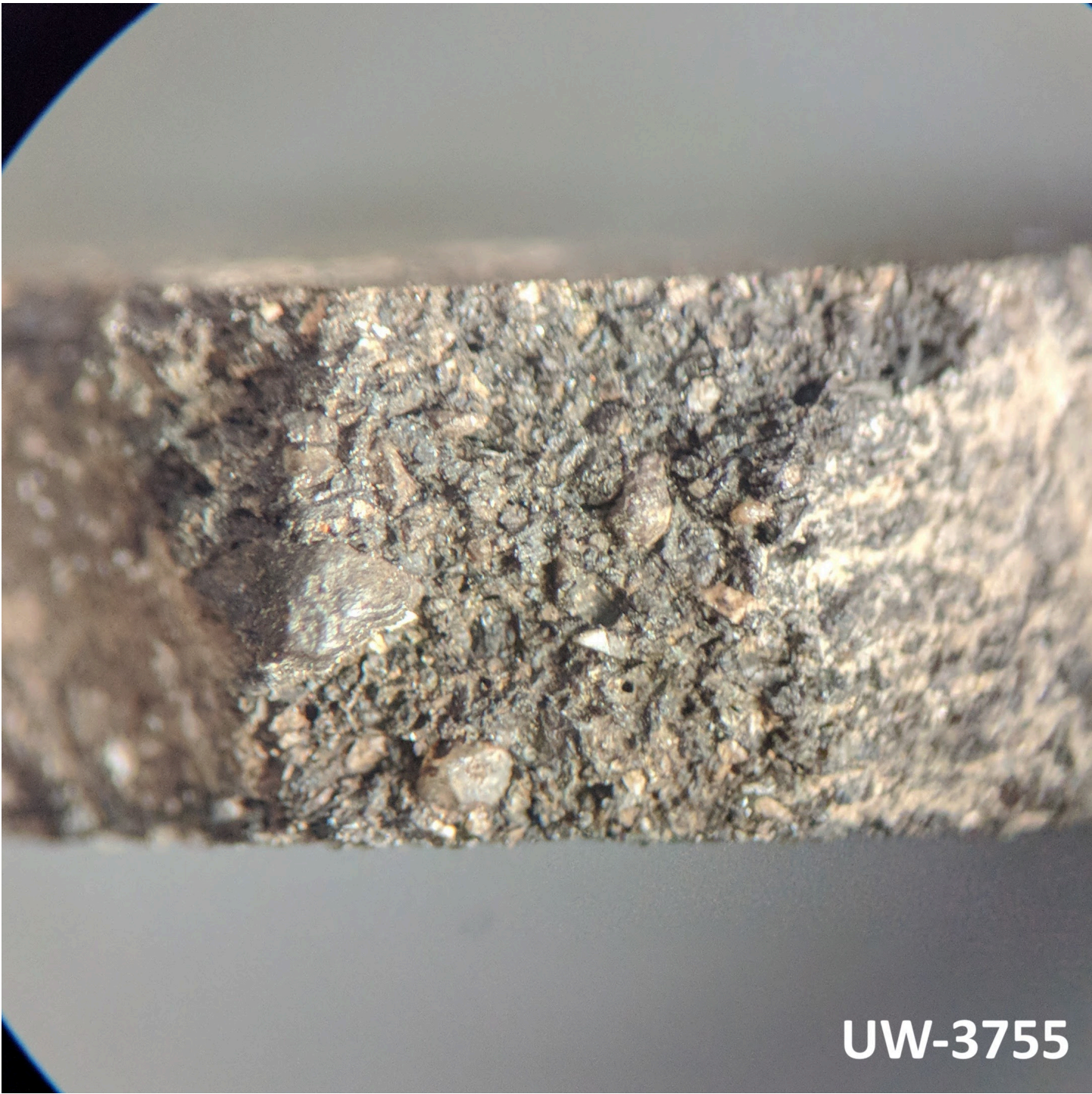
⑤

⑥

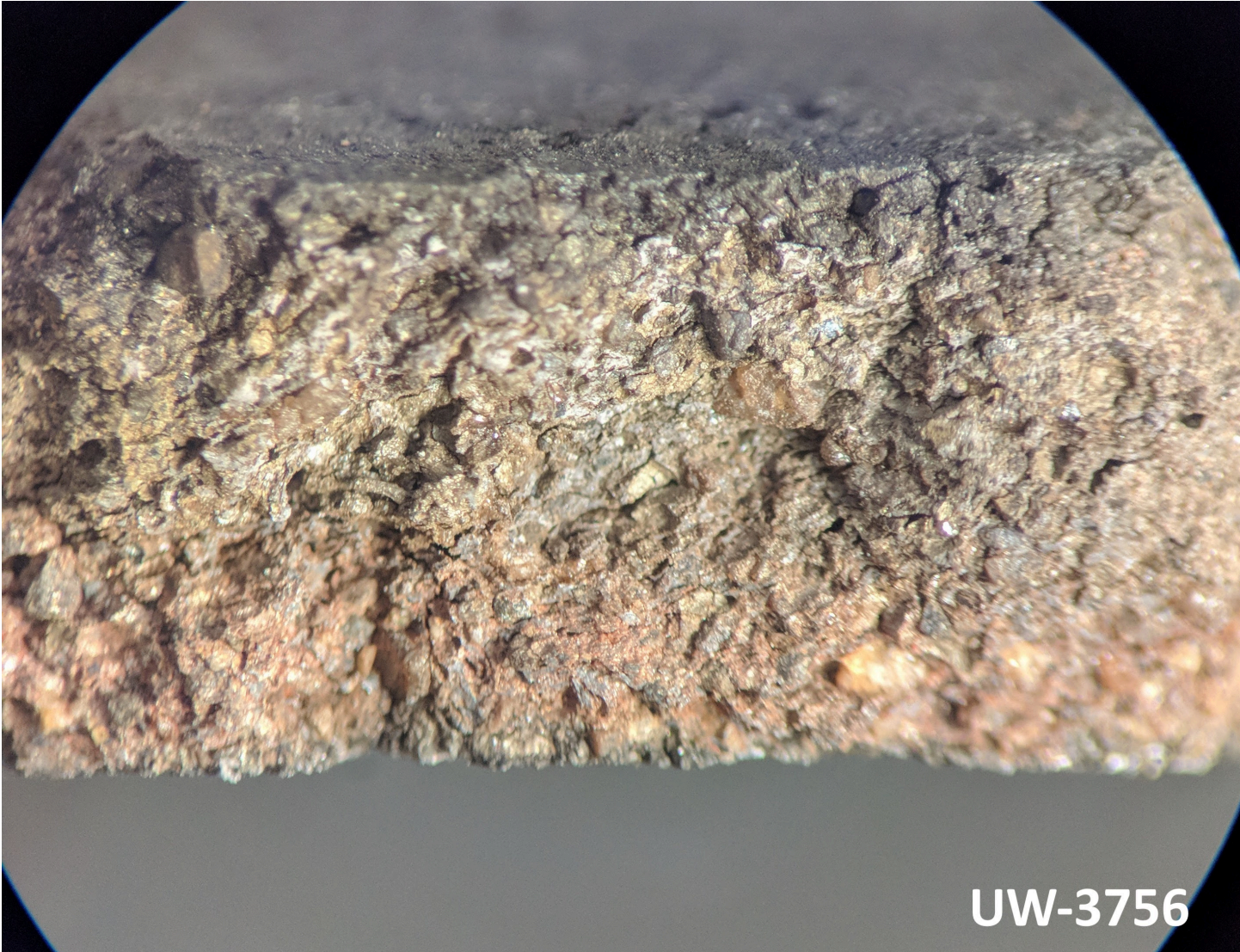




UW-3754



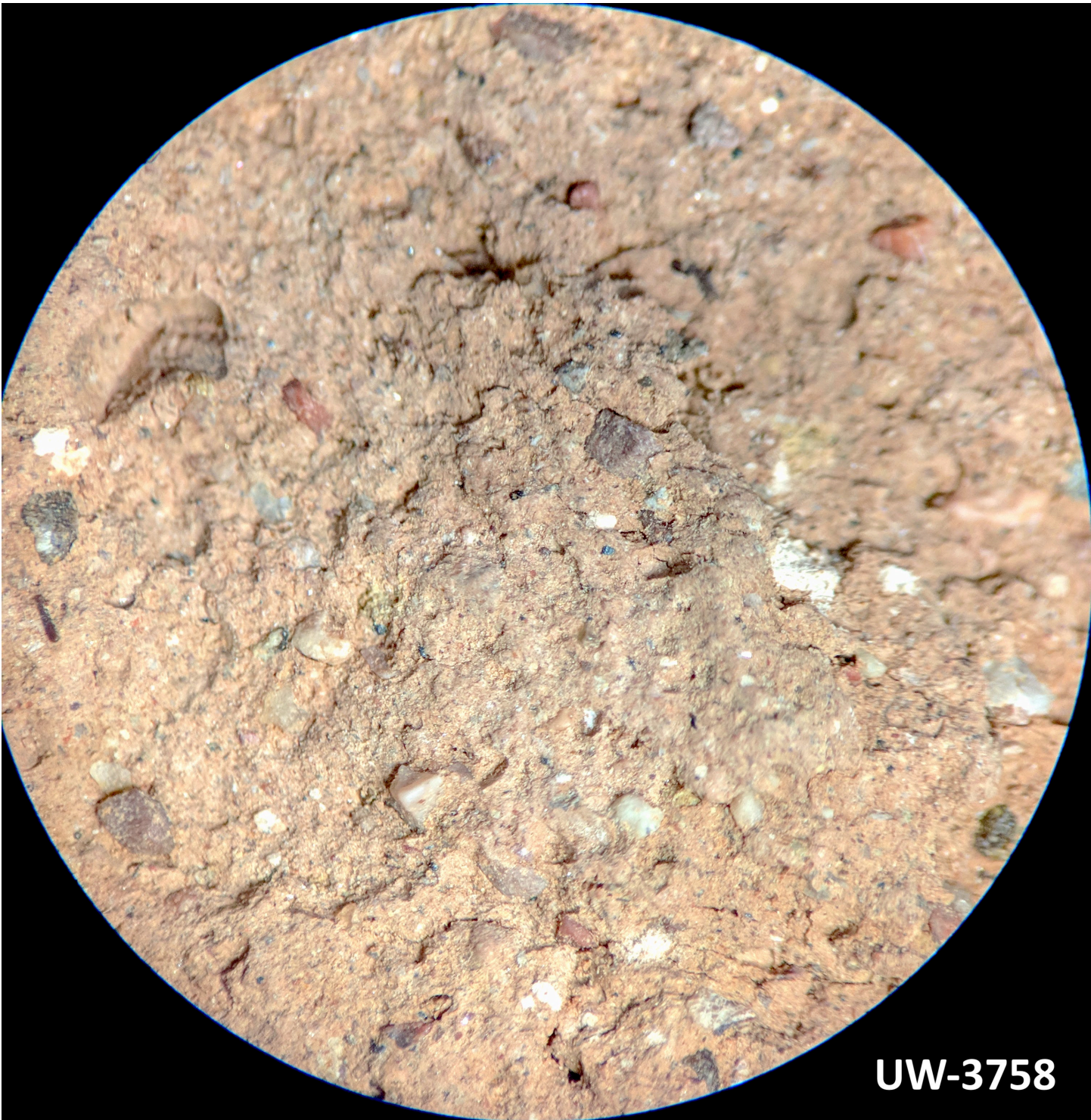
UW-3755



UW-3756



UW-3757



UW-3758

UW-3759

